Research Article

Ahmad Gholami, Mahdi Sedigh Shams, Abbas Abbaszadegan*, and Mohammadreza Nabavizadeh

Ionic liquids as capping agents of silver nanoparticles. Part II: Antimicrobial and cytotoxic study

https://doi.org/10.1515/gps-2021-0054
received March 13, 2021; accepted July 28, 2021

Abstract: This study was performed to validate the previous antimicrobial and cytotoxic data on the influence of ionic liquids as coatings of silver nanoparticles (AgNPs). The antibacterial and cytotoxicity assessments were carried out against different microorganisms and a cancerous cell line. AgNPs with two different ionic-liquid coatings and hydrocarbon chains were synthesized and characterized. We tested the antibacterial activity of these NPs against *Salmonella typhi*, *Bacillus subtilis*, *Staphylococcus aureus*, *Escherichia coli*, and *Candida albicans* in planktonic forms and against *Enterococcus faecalis* and *Escherichia coli* in biofilm forms. MTT (3-[4,5-dimethylthiazol-2-yl]-2,5 diphenyl tetrazolium bromide) assay was employed for toxicity evaluation. The antimicrobial activity of NPs with 12 carbons was significantly higher than those with 18 carbons. Furthermore, NPs with 12 carbons were also effective against bacterial biofilms. All of the NPs tested had good cell viability at different antimicrobial concentrations. The length of the hydrocarbon chain is an essential factor in determining the antimicrobial activity of ionic-liquid-coated AgNPs. The variation in ionic-liquid coatings was not as effective as other influencing factors. Evaluation of AgNPs using other alkyl chain lengths to find the optimal size is recommended.

Keywords: silver nanoparticles, antimicrobial, alkyl chain, charge, surface modification

1 Introduction

Owing to the indiscriminate use of antibiotics and the related multiple antibiotic resistance of pathogenic microorganisms, the need to search for new strategies to restrain these pathogens is essential [1,2].

Among different nanoparticles, silver nanoparticles (AgNPs) have shown antimicrobial features against a broad range of microorganisms, including Gram-positive bacteria, Gram-negative bacteria, and fungi [3–6]. AgNP antimicrobials refer to any silver-containing antimicrobial agent with nanoscale particles (smaller than 100 nm), with an enhanced activity because of their small particle sizes and significant active surface area [7]. It is shown that these agents demonstrate superior properties when particle sizes range between 5 and 50 nm [8].

The main proposed mechanisms of action for antimicrobial activity of AgNPs are the release of silver ions, generation of reactive oxygen, and damage to the cell membrane [9–11]. The positively charged NPs tend to attract negatively charged bacterial cell walls, causing them to accumulate inside the membrane, penetrate the cells, and eventually damage the bacterial cell walls [12,13].

Ionic liquids (ILs) are categorized as organic salts and are used as solvents consisting of polyatomic inorganic anions and organic cations. However, they are also used as electrolytes, and, therefore, considering their dual role, they can be marked as an environmental molecule with tunable ions. The application of ILs in green chemistry has been largely addressed in many aspects recently [14], where NPs are synthesized in organic solvents, achieving a good level of monodispersity and

* **Corresponding author: Abbas Abbaszadegan,** Department of Endodontics, Faculty of Dentistry, Shiraz University of Medical Sciences, Shiraz, Iran, e-mail: abbaszade@sums.ac.ir
Ahmad Gholami: Pharmaceutical Sciences Research Center, Faculty of Pharmacy, Shiraz University of Medical Sciences, P.O. Box 71345-1583, Shiraz, Fars, Iran; Biotechnology Research Center, Faculty of Pharmacy, Shiraz University of Medical Sciences, P.O. Box 71345-1583, Shiraz, Fars, Iran
Mahdi Sedigh Shams: Department of Endodontics, Faculty of Dentistry, Shiraz University of Medical Sciences, Shiraz, Iran
Mohammadreza Nabavizadeh: Department of Endodontics, Faculty of Dentistry, Shiraz University of Medical Sciences, Shiraz, Iran; Oral and Dental Disease Research Center, Faculty of Dentistry, Shiraz University of Medical Sciences, Shiraz, Iran

synthesis of particles with the same size and shape is highly probable. Moreover, the physical and chemical properties of ILs, such as hydrophobicity, viscosity, and polarity, can be changed by modifying their cations or anions, and the attached substituents such as alkyl chains. As an example, a strong association between the length of the alkyl chain in their structure and the level of polarity has been reported [15].

The coating of the AgNP surface with organic compounds such as ILs can inhibit particle aggregation and, therefore, enhance the positive charges at the surface of NPs thereby causing changes in the zeta potential value, which is defined as the potential difference between the surface of a solid particle immersed in a conducting liquid and the bulk of the liquid [16].

Considering these hypotheses, we initially examined the effect of charges on the surface of the imidazolium (Im)-coated AgNPs on their level of antimicrobial activity against different microorganisms. We found the positively charged Im-based AgNPs to be favorable antimicrobial agents with a low toxicity level [17,18]. Later, we tested another IL salt as a coating agent [pyridinium (Py)] in terms of antimicrobial activity and found that this substance was also able to change the bioactivity of AgNPs against *Enterococcus faecalis* [13].

Furthermore, we investigated the effect of the length and the number of alkyl chains attached to the IL coatings. We found that these parameters are capable of changing the characteristics of AgNPs, including the amount of surface charge, size, and bioactivity against *Enterococcus faecalis*. As a result, it was speculated that the regulation of the size of silver nuclei might be modulated by the alkyl chains [16,19].

It is known that the increase in the alkyl chain length can influence lipophilicity. Having said that, the higher lipophilicity may result in easier penetration of AgNPs into the cell membrane of the prokaryotic or eukaryotic cells, which, in turn, can affect the antibacterial activity and toxicity of NPs [20]. In other words, the greater repulsion between AgNPs with longer alkyl chains may lead to an increase in interparticle distances, decreasing aggregation and eventually promoting the efficacy of NPs [20].

Inspired by the promising results of Im-based AgNPs as a root canal irrigant, we also examined other features of this antimicrobial agent [21–23]. However, since our previous antimicrobial studies mainly were performed on *Enterococcus faecalis*, it was found relevant to validate our earlier results by observing the behavior of different AgNPs with positive charges, different coatings, and different alkyl chain lengths against a panel of microorganisms, including bacteria and a fungus. Therefore, this study was designed to validate the influence of the size of alkyl chain (12 hydrocarbons vs 18 hydrocarbon chain lengths) with different IL coatings on AgNP surfaces on antibacterial activity against a wide range of bacteria and fungi in both planktonic and biofilm forms and their relevant toxicity in human cells.

2 Materials and methods

2.1 Synthesis of NPs

The synthesis of ILs was carried out by reacting 1-methylimidazolium/pyridine with 1-chlorododecane/1-chlorooctane with no extra solvent in a flask fitted with a reflux condenser by heating and stirring the mixture at 70°C for about 48–72 h. Then, the temperature of the resultant liquid was decreased to 24°C and was washed using diethyl ether to obtain the ILs for the present experiment as 1-dodecyl-3-methylimidazolium chloride, 1-octadecyl-3-methylimidazolium chloride, 1-dodecyl pyridinium chloride, and 1-octadecyl pyridinium chloride.

For the synthesis of NPs, 1.0 mL of an aqueous solution of $AgNO_3$ (0.01 M) was mixed with 20 mL of each IL (6.2 mM) and stirred vigorously. The prepared 0.4 M $NaBH_4$ aqueous solution was then instantly added to the stirred solution drop by drop until a golden color was obtained. After that, the colloidal solutions were centrifuged for about 20 min to remove the unreacted ILs. The initial concentrations of all NP solutions before the commencement of the experiments were set as 1,024 μg/mL.

The four NP solutions prepared for this experiment were Im- and Py-protected with two different alkyl chains (C12, C18). AgNPs were characterized via a spectrophotometer (Ultrospec 3000 UV-Visible; Biochrom Ltd, Cambridge, UK) at a resolution of 1 nm. Additionally, transmission electron microscopy (TEM) analyses were performed on AgNPs at 200 kV, and then the average sizes of 250 particles were documented. The surface charges were also calculated via a zeta potential analyzer (Zeta Plus, Brookhaven Instruments, NY, USA).

2.2 Antimicrobial assessment

The test organisms were *Salmonella typhi* (PTCC 1609), *Bacillus subtilis* (PTCC 1720), *Staphylococcus aureus* (ATCC 29737), *Escherichia coli* (ATCC 15224), *Enterococcus faecalis* (PTCC1394), and *Candida albicans* (PTCC 5027).

Several antimicrobial assays including the zone of inhibition, minimum inhibitory concentration (MIC), minimum bactericidal concentration (MBC), and minimum biofilm inhibitory concentration (MBIC) were determined to assess the antibacterial activity. All experiments were performed in triplicate according to previous studies and based on the guidelines of the Clinical and Laboratory Standards Institute (CLSI) standards [24,25].

For the disc diffusion assay, 100 µL of each microbial suspension (1.5×10^8 CFU/mL) was separately spread on BHI (brain heart infusion) agar plates. After an incubation period of 24 h, 50 µL of each experimental solution was added in sterile blank 6-mm filter paper discs and lodged on the plates. After incubation for 24 h, the zone of inhibition was measured. Sterile normal saline was used as the negative control group.

For the MIC test, the two-fold serial dilution of all solutions up to seven times was prepared and poured into a 96-well microplate with Muller–Hinton broth (MHB) medium enriched with calcium (25 mg/L) and magnesium (12.5 mg/L) to a final volume of 90 µL. Afterward, 10 µL suspension of the test microorganism matching the turbidity of 2 McFarland standards was introduced to each microplate and subsequently incubated for 24 h at 37°C. The optical density of each microplate was determined using an ELISA reader (Biotek, Winooski, VT, USA) at an optical density of 600 nm. The minimum inhibitory concentration (MIC_{90}) was calculated where 90% of the bacterial growth was inhibited compared to the growth of the control group. The positive and negative control groups were microorganism-inoculated culture media and sterile culture media, respectively.

For the MBC test, the obtained concentrations of each solution those equal to or higher than MIC were selected to be spread on BHI agar plates. They were incubated overnight at 37°C, and the colonies were counted consequently.

The most effective NPs (NPs with 12 or 18 hydrocarbon chain lengths) were selected for a biofilm inhibition test and examined on a Gram-positive and a -negative bacterial species (*Enterococcus faecalis* and *Escherichia coli*). Microorganisms in BHI were contacted with a series of 2-fold dilutions in 96-well plates. After 24/48 h, the plates were rinsed two times with saline and 10% formaldehyde followed by a rewash with saline. Then, the biofilms were stained for 30 min using 0.5% crystal violet. The plates were cured with 200 µL of 2-propanol for 1 hand read via a microplate reader spectrophotometer at an optical density of 490 nm (VITA Easyshade; VITA Zahnfabrik, Bäd Sackingen, Germany). The absorbance of crystal violet is considered an indicator of the presence of a bacterial biofilm.

2.3 Cytotoxicity assessment

MTT [3-(4,5-dimethylthiazol-2-yl)-2,5-diphenyltetrazolium bromide] test was used to determine the cytotoxicity of the NP solutions on the MCF-7 cell line. Concisely, MCF-7 cells in PRMI1640 media were moved into a 96-well cell culture plate and incubated for 24 h at 37°C in 95% air in the presence of 5% CO_2.

The media was then refreshed with100 µL of each NP solution dissolved in RPMI1640 and incubated at 37°C for the second time. After 24 h, 25 µL of MTT solution (Sigma-Aldrich Co., St. Louis, MO, USA) was added to each well and incubated again for another 4 h with the previous experimental parameters. Furthermore, 100 µL of dimethyl sulfoxide was added to each well and incubated for 10 min. An ELISA plate reader (Biotek, Winooski, VT, USA) was employed to read the absorption of each NP solution at an optical density of 540 nm. The negative and positive control groups were culture media and hydrogen peroxide at a concentration of 35%, respectively. Cytotoxicity of Im and Py was also evaluated. All procedures were repeated three times for each group.

2.4 Statistical analysis

Statistical analysis was carried out using SPSS software (v 17.0) (SPSS Inc., Chicago, IL, USA).

The data from agar diffusion assays were analyzed using the Kruskal–Wallis test and then the Mann–Whitney *U* test for *post hoc* comparisons.

Cytotoxicity-related data were analyzed using one-way analysis of variance (ANOVA), and if the intergroup comparison test showed a significant difference, Tukey's Honestly Significant Difference (HSD) was carried out as a *post hoc* test. For all tests, the significance level was 5%.

3 Results

3.1 Characterization of NPs

In the UV-visible spectroscopy of the synthesized NPs (Figure 1), a characteristic peak at around λ 450 nm is seen which confirms the formation of AgNPs due to the reduction of Ag^+ ions into Ag^0.

The zeta potential distribution and the TEM images of the synthesized NPs are illustrated in Figures 2 and 3. The

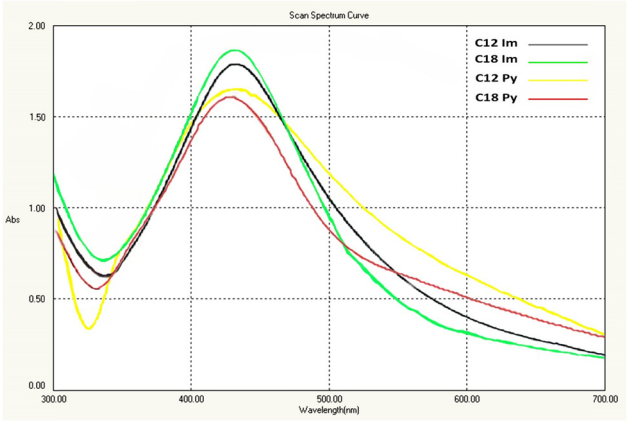

Figure 1: UV-visible spectroscopy of different ionic liquid-coated Ag nanoparticles.

surface charge density values (zeta/radius) of C12 Im, C18 Im, C12 Py, and C18 Py NPs were 5.55, 6.76, 1.35, and 8.58, respectively. Furthermore, the calculated sizes of particles were 9, 8.6, 18.49, and 6.71 nm for C12 Im, C18 Im, C12 Py, and C18 Py, respectively.

3.2 Antimicrobial activity of NPs

The disk diffusion test results revealed that C12 NPs had greater inhibition zones than C18 NPs, and the control group for all microorganisms was evaluated. The details are shown in Table 1.

Table 2 indicates the results of MIC and MBC of the tested NPs against each microorganism. The microdilution broth test verified that the C12 NPs killed planktonic microorganisms at lower concentrations compared to C18 NPs. Moreover, C12 NPs killed more than 90% of Gram-positive and -negative bacteria in the form of biofilms after 24 and 48 h, respectively (Figures 4–7).

3.3 Cytotoxic activity of NPs

The results exhibited that the level of cytotoxicity was concentration-dependent for all tested solutions (Table 3). NPs at 128 µg/mL or lower could retain the viability of 90% of MCF-7 cells in all groups. At higher concentrations, Py-based NPs showed more cytotoxicity, but the ANOVA test shows that the difference was not statistically significant for the concentrations examined.

4 Discussion

The study was performed to validate the previous data on the antimicrobial effect of alkyl chain length on the surface of AgNPs, along with the number of particle charges and its density (zeta/radius). The antibacterial activity of NPs was assessed against a panel of Gram-positive and -negative bacteria and a fungus. Besides, we evaluated their level of cytotoxicity in a mammalian cancer cell line. We verified that the length of the alkyl chain is an essential factor in determining antimicrobial activity, and the increase in the magnitude of the positive charge of AgNPs does not necessarily elevate the antimicrobial properties. Besides, all tested AgNPs were not cytotoxic to the MCF-7 cell line; however, at high concentrations, Im-coated NPs showed a lower cytotoxicity level than Py-coated NPs.

Resistance to antimicrobial agents, including antibiotics, has become a significant health problem in recent

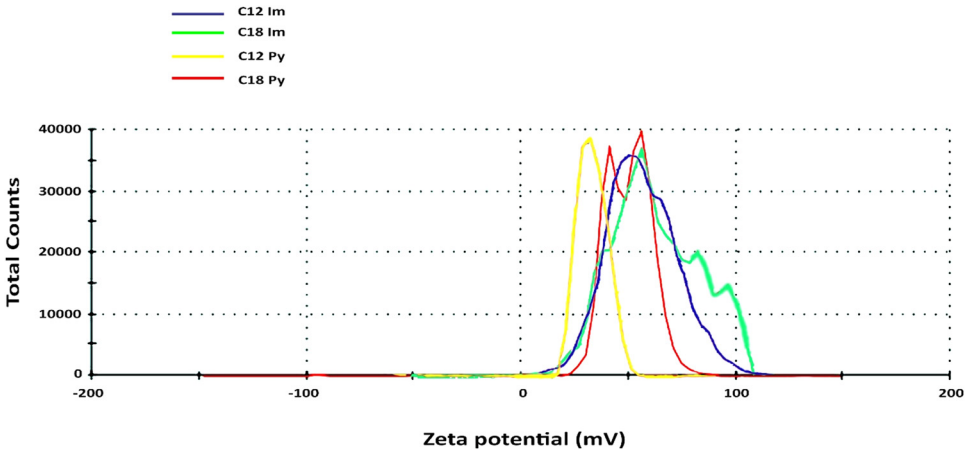

Figure 2: Zeta potential distribution of different ionic liquid-coated Ag nanoparticles.

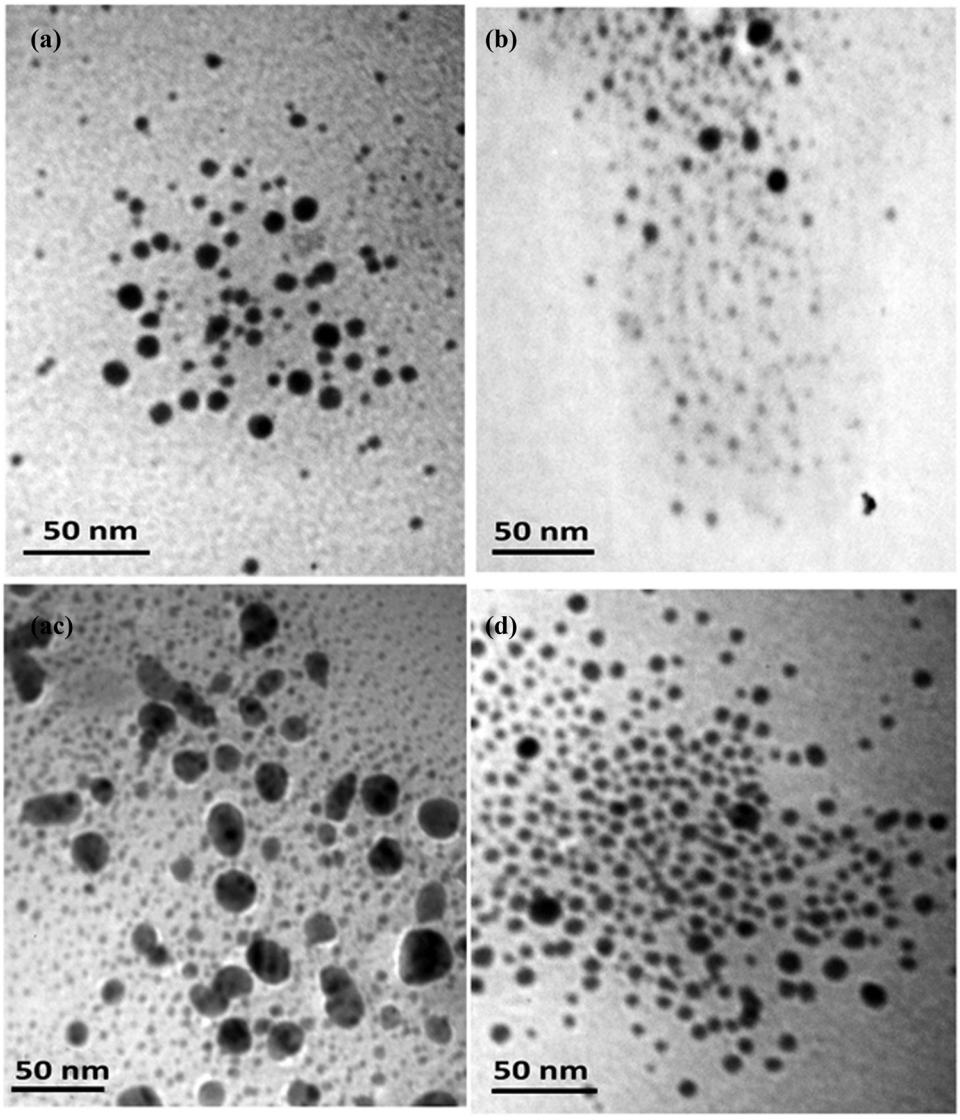

Figure 3: TEM images of nanoparticles: (a) C12 Im, (b) C18 Im, (c) C12 Py, and (d) C18 Py.

years [1]. To solve this problem, metallic NPs have been extensively studied for their antimicrobial properties. They have a high specific surface area and a high fraction of surface atoms, endowing them with unique physicochemical properties, including catalytic activity and electronic and magnetic properties [26]. Furthermore, the chance that bacteria develop resistance against metallic NPs is extremely less compared to other conventional and narrow-spectrum antibiotics [27]. It is because metals, especially silver, can act on a broad range of targets in microorganisms, and several mutations must occur in their genome to change this trait [27].

Table 1: Diameter of the inhibition zone in mm (median) against each microorganism

	C12 Im	C18 Im	C12 Py	C18 Py	*p*-value
Staphylococcus aureus	28^{A}	9^{B}	26^{A}	9^{B}	<0.01
Bacillus subtilis	25^{A}	8.5^{B}	23^{A}	10^{B}	0.01
Escherichia coli	20^{A}	4^{B}	16^{A}	0^{B}	<0.01
Salmonella typhi	17^{A}	0^{B}	18^{A}	0^{B}	0.04
Candida albicans	21^{A}	9.5^{B}	20^{A}	10^{B}	0.06

Different letters in a row indicate the presence of a statistically significant difference.

AgNPs should possess hydrophobicity to enhance their interactions with the cell membrane. On the other hand, hydrophilicity is also crucial for a steady dispersion in an aqueous solution to prevent aggregation [28]. As a result, a balance between these two features is

Table 2: The MIC and MBC of the tested nanoparticles against each microorganism

		C12 Im (μg/mL)	C18 Im (μg/mL)	C12 Py (μg/mL)	C18 Py (μg/mL)
Staphylococcus aureus	MIC	16	256	16	128
	MBC	16	256	16	128
Bacillus subtilis	MIC	16	512	16	256
	MBC	16	512	16	256
Escherichia coli	MIC	16	512	16	256
	MBC	16	512	16	256
Salmonella typhi	MIC	128	256	64	>512
	MBC	128	256	64	>512
Candida albicans	MIC	32	256	64	256
	MBC	32	256	64	256

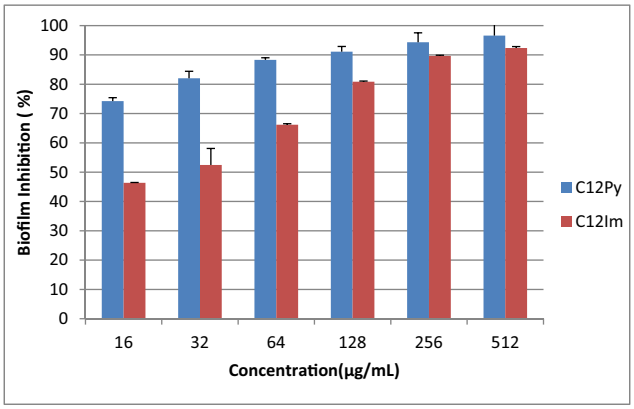

Figure 6: Inhibitory activity of C12 NPs at different concentrations against the biofilm formation of *Enterococcus faecalis* in 24 h.

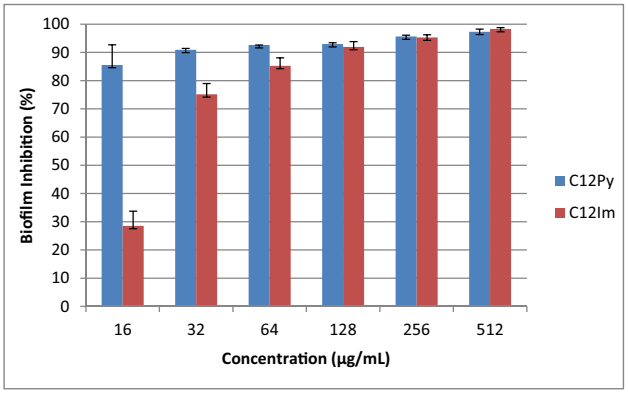

Figure 4: Inhibitory activity of C12 NPs at different concentrations against the biofilm formation of *Escherichia coli* in 24 h.

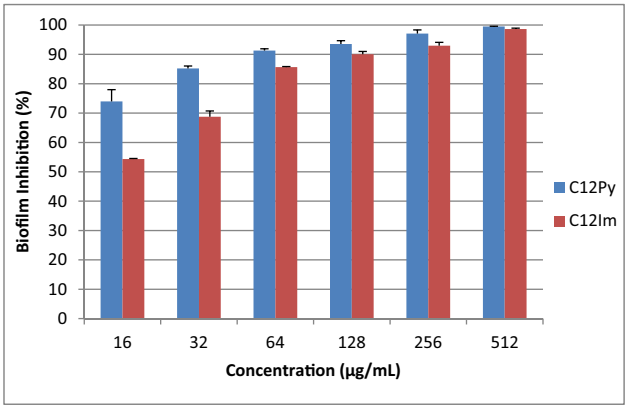

Figure 7: Inhibitory activity of C12 NPs at different concentrations against the biofilm formation of *Enterococcus faecalis* in 48 h.

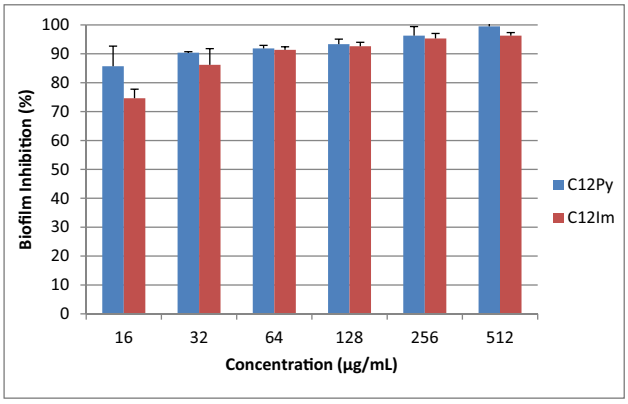

Figure 5: Inhibitory activity of C12 NPs at different concentrations against the biofilm formation of *Escherichia coli* in 48 h.

essential for a medicament to be effective against microorganisms. To gain hydrophobic characteristics, an alkyl chain was added to AgNPs. It should be noted that as the attached alkyl chain to AgNPs becomes longer, the hydrophobicity of NPs will increase. Furthermore, since the cell membrane is composed of phospholipids, containing a head group and a fatty acid tail that is roughly 10–20 hydrocarbons long [29], to obtain optimal results, the alkyl chain length was selected to be within this range.

We found that AgNPs with a shorter hydrocarbon length (C12) had increased antibacterial activity than longer-chain substitutes (C18) against all tested microorganisms. Agar diffusion and microdilution broth tests revealed that C12 AgNPs had a more significant inhibition zone and could kill microorganisms at lower concentrations. This finding was regardless of the type of IL used. This effect might be due to the low hydrophobicity of C18 particles, which had an adverse effect on their dispersion and, in turn, their antibacterial efficacy.

Given that the cellular membrane of the bacteria has a negative charge due to the presence of phosphate,

Table 3: The viability of MCF-7 cells (%) when treated with different concentrations of the tested nanoparticles (mean ± SD)

Concentration (μg/mL)	C12 Im	C18 Im	C12 Py	C18 Py	*p*-value
512	94.46 ± 14.42	85.82 ± 13.89	74.46 ± 7.40	69.04 ± 14.68	0.151
256	95.12 ± 11.46	89.51 ± 13.59	88.67 ± 9.34	79.34 ± 12.29	0.472
128	97.58 ± 5.15	93.25 ± 12.11	94.42 ± 5.22	87.71 ± 5.33	0.488
64	106.61 ± 6.22	102.09 ± 7.93	97.66 ± 12.90	93.78 ± 18.59	0.633
32	101.55 ± 8.25	101.50 ± 4.09	102.40 ± 14.59	99.14 ± 11.58	0.982
16	101.22 ± 7.21	103.80 ± 9.91	102.12 ± 11.56	101.57 ± 3.04	0.982

carboxyl, and amino groups, particles with positive charge have more tendency to attack the bacterial membrane [12,30]. However, we found that the increase in the positive charge of AgNPs does not necessarily elevate antimicrobial properties. Although C12 Py-coated NPs had the least surface area and density of charge among the tested AgNPs, they showed better antimicrobial activity than other NPs in general. This may be interpreted due to the fact that an increase in the number of particles with the same charge can result in the repulsion of the particles from each other and an increase in the distance between them, and, therefore, it may have an adverse effect on the level of antimicrobial activity. Hence, we propose that a balance between lipophilicity and hydrophobicity is a more influential factor for antibacterial activity and might be a more critical factor than the density of surface charges.

Previous studies have confirmed that in the case where NPs bear surface groups with a positive charge, even a slight change in surface functionalities can change the degree of hydrophobicity, resulting in varying amounts of internalization in the cells [31,32]. For instance, Zue et al. [31] demonstrated that among gold NPs that had positive charges, most hydrophobic NPs were the least efficient NPs taken up by the monkey kidney cells. This was inconsistent with our findings that hydrophobic AgNPs with more extended chain coatings were less effective and could be because they were less taken up by microbial cells.

Our research team previously found that AgNPs coated with Py killed *Enterococcus faecalis* better than those coated with Im. However, in the current study, the antimicrobial test results were dissimilar in terms of the microorganisms tested and alkyl chain lengths. AgNPs with a 12-hydrocarbon chain length showed enhanced antimicrobial activity. Considering these results together, the type of IL coating might not be as effective as the alkyl chain length in determining antimicrobial features of AgNPs.

In this study, only C12 NPs were assessed for antibacterial activity against biofilms as they are more hydrophilic than C18 counterparts and had better results against planktonic bacteria. Given that the virulent biofilms are the cause of the majority of persistent human infectious diseases [33], and the extracellular polymeric substance (EPS) matrix is strongly anionic, positive NPs can penetrate this matrix more efficiently compared to the uncharged or anionic counterparts based on a catch-and-release phenomenon [34]. Furthermore, when NPs enter the biofilm, their hydrophilicity is crucial because microorganisms take up hydrophobic NPs, but hydrophilic cationic particles remain bound to the EPS [34].

Although the Py-coated NPs are less cationic than Im-coated ones, for both *Escherichia coli* and *Enterococcus faecalis*, Py-coated NPs inhibited the formation of their biofilms more effectively than Im-coated ones after 24 h, especially at lower concentrations. Nevertheless, after 48 h, the difference narrowed, but Py-coated NPs were still more effective. As discussed earlier, this can be interpreted by the fact that when molecules become more cationic, they repel each other more strongly. On the other hand, they attach more tightly to EPS and make their release to bacterial cells more difficult.

The toxicity of an antimicrobial agent is also an important aspect that needs to be evaluated because these agents are in direct contact with human tissues. This evaluation is even more critical for cationic NPs because they distribute more through nonphagocytic cells and are more toxic [35]. However, the current study showed that the alteration in the magnitude of the positive charges on the surface of AgNPs may not result in an increase in the level of cytotoxicity. For example, C12 Py-coated NPs, at high concentrations (512 μg/mL), did not show lower toxicity than other tested NPs. However, they have higher zeta potential values compared to other NPs. Although the differences were not statistically significant at higher concentrations, Im-coated NPs showed lower toxicity than Py-coated counterparts. *In vivo* studies are required to evaluate tissue reaction to these materials and to validate our findings.

Future studies can be targeted at the synthesis of NPs coated with a combination of hydrophobic and

hydrophilic carriers to enable them to penetrate the cell membrane and easily dissolve in water.

5 Conclusion

Within the limitations of this study, we found that the alkyl length is an essential factor in determining the antimicrobial activity of AgNPs. However, modification in IL coatings was not as effective as other influencing factors considered in this study. We suggest evaluating NPs with different alkyl chain lengths, such as NPs with 10, 14, or 16 hydrocarbons, to find the optimal hydrocarbon chain length.

Acknowledgment: The authors thank the Vice-Chancellery of Shiraz University of Medical Sciences for supporting this research (Grant #23092). The authors would also like to thank Dr Mehrdad Vosooghi of the Research Development Center for the statistical analysis.

Funding information: This research received funding from the Shiraz University of Medical Sciences.

Author contributions: Ahmad Gholami: conceptualization, data curation, methodology, visualization, project administration, writing – original draft, writing – review and editing; Mahdi Sedigh Shams: conceptualization, data curation, writing – original draft, formal analysis, visualization, project administration; Abbas Abbaszadegan: conceptualization, data curation, writing – original draft, writing – review and editing, visualization, project administration; Mohammad Reza Nabavizadeh: resources, data curation, methodology, validation, writing – original draft, writing – review and editing.

Conflict of interest: The authors state no conflict of interest.

Data availability statement: The datasets generated during the current study are available from the corresponding author on reasonable request.

References

[1] Wang L, Hu C, Shao L. The antimicrobial activity of nanoparticles: present situation and prospects for the future. Int J Nanomed. 2017;12:1227.

[2] Moazami F, Gholami A, Mehrabi V, Ghahramani Y. Evaluation of the antibacterial and antifungal effects of ProRoot MTA and nano-fast cement: an in vitro study. J Contemp Dent Pract. 2020;21(7):761.

[3] Al-thabaiti SA, Khan Z, Manzoor N. Biosynthesis of silver nanoparticles and its antibacterial and antifungal activities towards Gram-positive, Gram-negative bacterial strains and different species of Candida fungus. Bioprocess Biosyst Eng. 2015;38(9):1773–81.

[4] Mohammadi F, Abbaszadegan A, Gholami A. Recent advances in nanodentistry: a special focus on endodontics. Micro Nano Lett. 2020;15(12):812–6.

[5] Chartarrayawadee W, Charoensin P, Saenma J, Rin T, Khamai P, Nasomjai P, et al. Green synthesis and stabilization of silver nanoparticles using Lysimachia foenum-graecum Hance extract and their antibacterial activity. Green Process Synth. 2020;9(1):107–18.

[6] Kumar A, Madhu G, John E, Kuttinarayanan S, Nair S. Optical and antimicrobial properties of silver nanoparticles synthesized via green route using honey. Green Process Synth. 2020;9(1):268–74.

[7] Miernicki M, Hofmann T, Eisenberger I, von der Kammer F, Praetorius A. Legal and practical challenges in classifying nanomaterials according to regulatory definitions. Nat Nanotechnol. 2019;14(3):208–16.

[8] Alt V, Bechert T, Steinrücke P, Wagener M, Seidel P, Dingeldein E, et al. An in vitro assessment of the antibacterial properties and cytotoxicity of nanoparticulate silver bone cement. Biomaterials. 2004;25(18):4383–91.

[9] Durán N, Durán M, De Jesus MB, Seabra AB, Fávaro WJ, Nakazato G. Silver nanoparticles: a new view on mechanistic aspects on antimicrobial activity. Nanomedicine. 2016;12(3):789–99.

[10] Marambio-Jones C, Hoek EM. A review of the antibacterial effects of silver nanomaterials and potential implications for human health and the environment. J Nanopart Res. 2010;12(5):1531–51.

[11] Gholami A, Mohammadi F, Ghasemi Y, Omidifar N, Ebrahiminezhad A. Antibacterial activity of SPIONs versus ferrous and ferric ions under aerobic and anaerobic conditions: a preliminary mechanism study. IET Nanobiotechnol. 2019;14(2):155–60.

[12] Abbaszadegan A, Ghahramani Y, Gholami A, Hemmateenejad B, Dorostkar S, Nabavizadeh M, et al. The effect of charge at the surface of silver nanoparticles on antimicrobial activity against gram-positive and gram-negative bacteria: a preliminary study. J Nanomater. 2015;2015:720654.

[13] Abbaszadegan A, Nabavizadeh M, Gholami A, Aleyasin Z, Dorostkar S, Saliminasab M, et al. Positively charged imidazolium-based ionic liquid-protected silver nanoparticles: a promising disinfectant in root canal treatment. Int Endod J. 2015;48(8):790–800.

[14] Mallakpour S, Dinari M. Ionic liquids as green solvents: progress and prospects. In: Mohammad A, Inamuddin D, editors. Green solvents II. Dordrecht: Springer; 2012. p. 1–32.

[15] Carmichael AJ, Seddon KR. Polarity study of some 1-alkyl-3-methylimidazolium ambient-temperature ionic liquids with the solvatochromic dye, Nile Red. J Phys Org Chem. 2000;13:591–5.

[16] Yamamoto M, Kashiwagi Y, Nakamoto M. Size-controlled synthesis of monodispersed silver nanoparticles capped by long-chain alkyl carboxylates from silver carboxylate and tertiary amine. Langmuir. 2006;22(20):8581–6.
[17] Nabavizadeh M, Abbaszadegan A, Gholami A, Kadkhoda Z, Mirhadi H, Ghasemi Y, et al. Antibiofilm efficacy of positively charged imidazolium-based silver nanoparticles in Enterococcus faecalis using quantitative real-time PCR. Jundishapur J Microbiol. 2017;10:10.
[18] Nabavizadeh M, Ghahramani Y, Abbaszadegan A, Jamshidzadeh A, Jenabi P, Makarempour A. In vivo biocompatibility of an ionic liquid-protected silver nanoparticle solution as root canal irrigant. Iran Endod J. 2018;13(3):293.
[19] Kashiwagi Y, Yamamoto M, Nakamoto M. Facile size-regulated synthesis of silver nanoparticles by controlled thermolysis of silver alkylcarboxylates in the presence of alkylamines with different chain lengths. J Colloid Interface Sci. 2006;300(1):169–75.
[20] Abbaszadegan A, Gholami A, Abbaszadegan S, Aleyasin ZS, Ghahramani Y, Dorostkar S, et al. The effects of different ionic liquid coatings and the length of alkyl chain on antimicrobial and cytotoxic properties of silver nanoparticles. Iran Endod J. 2017;12(4):481.
[21] Abbaszadegan A, Ghahramani Y, Farshad M, Sedigh-Shams M, Ghomali A, Jamshidzadeh A. In vitro evaluation of dynamic viscosity, surface tension and dentin wettability of silver nanoparticles as an irrigation solution. Iran Endod J. 2018;14(1):23–7.
[22] Adl A, Abbaszadegan A, Gholami A, Parvizi F, Ghahramani Y. Effect of a new imidazolium-based silver nanoparticle irrigant on the bond strength of epoxy resin sealer to root canal dentine. Iran Endod J. 2019;14(2):122–5.
[23] Ghahramani Y, Yaghoubi F, Motamedi R, Jamshidzade A, Abbaszadegan A. Effect of endodontic irrigants and medicaments mixed with silver nanoparticles against biofilm formation of enterococcus faecalis. Iran Endod J. 2018;13(4):559–64.
[24] Clinical and Laboratory Standards Institute (CLSI). Performance standards for antimicrobial susceptibility testing; twenty-fourth informational supplement. CLSI document M100-S24. Wayne, PA: Clinical and Laboratory Standard Institute; 2014.
[25] Abbaszadegan A, Sahebi S, Gholami A, Delroba A, Kiani A, Iraji A, et al. Time-dependent antibacterial effects of Aloe vera and Zataria multiflora plant essential oils compared to calcium hydroxide in teeth infected with Enterococcus faecalis. J Investig Clin Dent. 2016;7(1):93–101.
[26] Shahverdi AR, Fakhimi A, Shahverdi HR, Minaian S. Synthesis and effect of silver nanoparticles on the antibacterial activity of different antibiotics against Staphylococcus aureus and Escherichia coli. Nanomedicine. 2007;3(2):168–71.
[27] Pal S, Tak YK, Song JM. Does the antibacterial activity of silver nanoparticles depend on the shape of the nanoparticle? A study of the gram-negative bacterium Escherichia coli. Appl Environ Microbiol. 2007;73(6):1712–20.
[28] Fratoddi I. Hydrophobic and hydrophilic Au and Ag nanoparticles. Breakthroughs and perspectives. Nanomaterials. 2018;8(1):11.
[29] Milo R, Phillips R. Cell biology by the numbers. New York , USA: Garland Science; 2015.
[30] Gholami A, Shahin S, Mohkam M, Nezafat N, Ghasemi Y. Cloning, characterization and bioinformatics analysis of novel cytosine deaminase from Escherichia coli AGH09. Int J Pept Res Ther. 2015;21(3):365–74.
[31] Zhu Z-J, Ghosh PS, Miranda OR, Vachet RW, Rotello VM. Multiplexed screening of cellular uptake of gold nanoparticles using laser desorption/ionization mass spectrometry. J Am Chem Soc. 2008;130(43):14139–43.
[32] Verma A, Stellacci F. Effect of surface properties on nanoparticle–cell interactions. Small. 2010;6(1):12–21.
[33] Benoit DS, Sims Jr KR, Fraser D. Nanoparticles for oral biofilm treatments. ACS Nano. 2019;13(5):4869–75.
[34] Li X, Yeh Y-C, Giri K, Mout R, Landis RF, Prakash Y, et al. Control of nanoparticle penetration into biofilms through surface design. ChemComm. 2015;51(2):282–5.
[35] Fröhlich E. The role of surface charge in cellular uptake and cytotoxicity of medical nanoparticles. Int J Nanomed. 2012;7:5577.